

# X-ray stress analysis technique using the optimization of $d_0$ with error term

## Direct Refinement Solution (DRS) method

Shoichi Yasukawa\*

### 1. Introduction

Stress analysis using X-ray diffraction is a well-known, effective technique for nondestructive evaluation of residual stresses in the surface of materials. Among X-ray stress analyses, the  $\sin^2\psi$  method<sup>(1)</sup> is the most widely used and very common, especially in the industrial field. In this method, residual stress is calculated by assuming a plane stress condition as the stress state on the surface of materials. In detail, it is calculated by multiplying the X-ray stress constant specific to materials by the slope of a regression line between observed diffraction angle ( $2\theta$ ) and the  $\sin^2\psi$  function. As a result, it is not necessary to obtain the information on crystal lattice spacing (d-value) in the strain-free condition  $d_0$ , which is very difficult to know beforehand. This is why use of the  $\sin^2\psi$  method has become widespread as an effective analysis method.

On the other hand, in manufacturing processes such as surface modification, thermal processing, and fabrication, the stresses applied to the surface of materials may not only be an equi-biaxial stress state but also a biaxial or a triaxial stress state. Therefore, the need for more accurate inspection or evaluation of the stress state in the surface of materials is increasing; namely, biaxial or triaxial stress analysis is strongly required.

The Direct Refinement Solution (DRS) method proposed here is an effective technique for biaxial or triaxial stress analysis. This method calculates stresses using an equation that most faithfully represents the relationship between stress and strain in isotropic elastic bodies.

Since the stress state on the surface of actual materials must be assumed for the stress calculation, the DRS method has been developed to improve accuracy in the calculations. As one of its applications, this method is capable of analyzing stresses on the basis of a single Debye-Scherrer obtained by the single exposure technique. This technique is employed in our new portable X-ray stress analyzer SmartSite RS, designed for on-site measurements that require compact and lightweight analyzers and a short measurement time.

### 2. X-ray diffraction and stress

#### 2.1. Stress state and stress tensor

A region to which stresses are applied is referred to as the “stress field”, and the state; *i.e.* how stresses are applied to the region, is referred to as the “stress state”. The stress state is represented by a second-order tensor  $\sigma_{ij}$  ( $i, j=1, 2, 3$ ) that is composed of the stresses applied to a microcube at an arbitrary point within the stress field. The first suffix “ $i$ ” of the stress tensor denotes the plane to which the stress is applied, and the second suffix denotes the direction in which the stress is applied. For example,  $\sigma_{11}$  is a component that is applied to a plane perpendicular to the x axis in the x-axis direction. This type of stress component is referred to as “normal stress”. Likewise,  $\sigma_{23}$  is a component that is applied to a plane perpendicular to the y axis in the z-axis direction. This type of component is referred to as “shear stress”. Since all stresses applied to an arbitrary point within a stress field are balanced, shear stresses are represented by  $\sigma_{ij} = \sigma_{ji}$ . Thus, it follows that stress tensors are symmetric.

#### 2.2. Principal stress

The axes represented by eigenvectors of a stress tensor are referred to as the “principal axes of stress”, and the eigenvalues are referred to as the “principal stresses”. On the principal axes, all components of shear stresses are zero. The stress state in which all principal

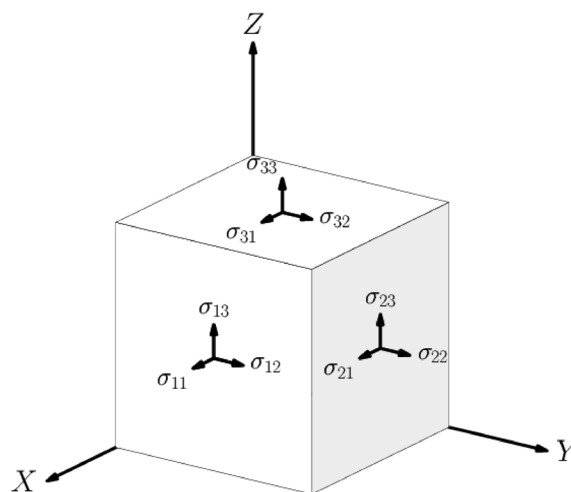
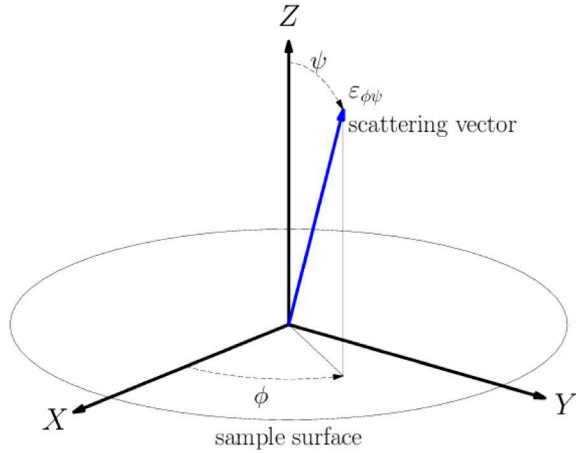


Fig. 1. Stress tensor.

\* SBU PDX, X-ray Instrument Division, Rigaku Corporation.



**Fig. 2.** A coordinate system for stress analysis using X-ray diffraction.

stresses are non-zero is referred to as the “triaxial stress state”. In the triaxial stress state, stresses are applied to a certain point from all directions. In contrast, the stress state in which one of the principal stresses is zero is referred to as the “biaxial stress state” or the “plane stress state”. Moreover, if the absolute values of the applied stress vectors within the biaxial stress state are all equal, the state is referred to as the “equi-biaxial stress state”.

The stress vectors applied to a certain point in a biaxial stress state are distributed on a plane based on the principal axis including that point. This type of plane is referred to as the “principal stress plane”. According to the definition of the biaxial stress state, a principal stress plane can intersect with a material surface at arbitrary angles. However, due to the following reason, a principal stress plane is parallel to the material surface in the region near the surface that can be observed by X-ray diffraction.

Since a material surface is open-ended, no normal stress can exist on it. Let us denote the absolute value of the normal stress vector to this material surface observed by X-ray diffraction as  $\sigma_N$ . Since the value is the weighted average of the range from the material surface to several  $\mu\text{m}$  in depth, it can only be extremely small, even if the stresses are distributed in the depth direction. If biaxial stress states exist on a material surface and their principal stress planes are not parallel to the material surface, a stress component orthogonal to the principal stress plane must exist in order to satisfy  $\sigma_N \cong 0$ . This is inconsistent with the definition of biaxial stress state. Therefore, the principal stress planes in biaxial stress states that exist near a material surface must be parallel to the material surface.

### 2.3. Stress analysis using X-ray diffraction

Let us define a Cartesian coordinate system with its X, Y axes on an isotropic elastic material surface and the Z axis in the normal to the surface. Assuming that the angle formed by an X-ray scattering vector and the Z axis is  $\psi$ , and the angle formed by the projection on

the material surface of the X-ray scattering vector and the X axis is  $\phi$ , the normal strain  $\varepsilon_{\phi\psi}$  observed from the direction of the X-ray scattering vector is represented by the following equation using the normal stress and shear stress on each coordinate axis.

$$\varepsilon_{\phi\psi} = \frac{1}{2} S_2 \{ (\sigma_{11} \cos^2 \phi + \sigma_{12} \sin 2\phi + \sigma_{22} \sin^2 \phi) \sin^2 \psi + (\sigma_{13} \cos \phi + \sigma_{23} \sin \phi) \sin 2\psi + \sigma_{33} \cos^2 \psi \} + S_1 (\sigma_{11} + \sigma_{22} + \sigma_{33}) \quad (1)$$

where,  $S_1$  and  $S_2$  are constants called “X-ray Elastic Compliance”. These constants are given by using Young’s modulus  $E$  and Poisson’s ratio  $\nu$  as below.

$$S_1 = -\frac{\nu}{E} \quad (2)$$

$$\frac{1}{2} S_2 = \frac{1+\nu}{E} \quad (3)$$

On the other hand, the d-value can be measured using X-ray diffraction. Defining  $d_{\phi\psi}$  as a d-value measured with an X-ray optical system aligned so that the scattering vector, namely the normal of its targeting crystal lattice plane, is directed in the orientation indicated by  $\phi$  and  $\psi$ , and  $d_0$  as the d-value in strain-free condition,  $\varepsilon_{\phi\psi}$  is represented by

$$\varepsilon_{\phi\psi} = \frac{d_{\phi\psi} - d_0}{d_0} \quad (4)$$

Since  $d_0$  is a unique value for each material,  $\sigma_{11}$ ,  $\sigma_{22}$ ,  $\sigma_{33}$  and  $\sigma_{23}$ ,  $\sigma_{13}$ ,  $\sigma_{12}$  can be theoretically obtained from d-values measured in six or more pairs of  $\phi$  and  $\psi$ .

However, in reality,  $d_0$  varies easily depending on the state, such as crystal polymorph and solid solution, and thus it is difficult to know the accurate value of  $d_0$  for all samples beforehand. Therefore, if stress values are calculated using the given  $d_0$  and Eq. (1) directly, the results may contain large errors due to the following reason.

The d-value in the strain-free condition containing errors  $d_{0(k)}$  is defined as below.

$$d_{0(k)} = d_0 (1 + \Delta_{(k)}) \quad (5)$$

The strain containing errors  $\varepsilon_{\phi\psi(k)}$  calculated from  $d_{0(k)}$  and  $d_{\phi\psi}$  using Eq. (1) is defined by

$$\varepsilon_{\phi\psi(k)} = \varepsilon_{\phi\psi} + \Delta_{\varepsilon(k)} \quad (6)$$

From Eq. (5) and (6), we obtain

$$\begin{aligned} \varepsilon_{\phi\psi(k)} &= \frac{d_{\phi\psi} - d_{0(k)}}{d_{0(k)}} \\ \varepsilon_{\phi\psi} + \Delta_{\varepsilon(k)} &= \frac{d_{\phi\psi}}{d_0 (1 + \Delta_{(k)})} - 1 \\ &\cong \frac{d_{\phi\psi}}{d_0} (1 - \Delta_{(k)}) - 1 \end{aligned} \quad (7)$$

$$\begin{aligned} \therefore \Delta_{\varepsilon(k)} &\cong -\frac{d_{\varphi\psi}}{d_0} \Delta_{(k)} \\ &\cong -\Delta_{(k)} \end{aligned} \quad (8)$$

Since the value of  $\varepsilon_{\varphi\psi}$  is less than  $10^{-3}$ ,  $\Delta_{\varepsilon}$  may be several times as large as  $\varepsilon_{\varphi\psi}$ , when  $\Delta_{(k)}$  is not so small, e.g.,  $\Delta_{(k)}$  is on the order of  $10^{-2}$ . In this case, errors in stress values calculated from strains containing such errors will also contain errors that are several times as large as the true values.

As a method to avoid such calculation errors attributed to the errors contained in  $d_0$ , it is considered to calculate not only the six components of the stress tensors but also  $d_0$ , given as a variable in the following non-linear equation, using the d-values that were obtained by seven or more pairs of  $\varphi$  and  $\psi$ .

$$d_{\varphi\psi} = d_0 \left\{ \varepsilon_{\varphi\psi} (\sigma_{ij}) + 1 \right\} \quad (9)$$

However, all six components of a stress tensor and  $d_0$  cannot be obtained even by using Eq. (9), due to the following reason. If the right-hand side of Eq. (9) is placed in Eq. (10), it becomes a nonlinear equation, as below.

$$f(d_0, \sigma_{ij}) = d_0 \left\{ \varepsilon_{\varphi\psi} (\sigma_{ij}) + 1 \right\} \quad (10)$$

In the case of either solving Eq. (10) or obtaining the optimal solution for  $d_{\varphi\psi}$  of eight or more pairs using a least squares method, the following linear simultaneous Eq. (11) must be repeatedly solved to obtain the error values  $\Delta d_{0(k)}$ ,  $\Delta \sigma_{ij(k)}$  used to improve the appropriately given provisional values  $d_{0(k)}$ ,  $\sigma_{ij(k)}$ .

$$d_{\varphi\psi} - f(d_{0(k)}, \sigma_{ij(k)}) = \left( \frac{\partial f}{\partial d_0} \quad f \right) \begin{pmatrix} \Delta d_{0(k)} \\ \Delta \sigma_{ij(k)} \end{pmatrix} \quad (11)$$

$\frac{\partial f}{\partial d_0}$  in the coefficients of Eq. (11) is expressed as below.

$$\frac{\partial f}{\partial d_0} = \varepsilon_{\varphi\psi} (\sigma_{ij(k)}) + 1 \quad (12)$$

This value is the sum of a linear combination of other coefficients and a constant. On the other hand, the following relationship is established in the coefficients of Eq. (11) regardless of the values of  $\varphi$  and  $\psi$ .

$$\frac{\partial f}{\partial \sigma_{11}} + \frac{\partial f}{\partial \sigma_{22}} + \frac{\partial f}{\partial \sigma_{33}} = d_{0(k)} \left( \frac{1}{2} S_2 + 3S_1 \right) \quad (13)$$

The right-hand side of Eq. (13) is a constant. Thus, Eq. (11) cannot be solved because the column vectors of its coefficient matrix become linearly dependent. For this reason and the large errors attributed to the errors contained in  $d_0$  mentioned above, it is quite difficult to obtain all components of a stress tensor in any stress state by using X-ray diffraction and Eq. (1) directly.

#### 2.4. Analysis method with a strain error term

Using X-ray diffraction, we can obtain information on the stress states only in a region near the surface of

materials. In this region,  $\sigma_{33}$  can be regarded as zero or a small constant in some cases. If so, Eq. (13) does not hold, and the values of  $d_0$  and the components other than  $\sigma_{33}$  of a stress tensor can be obtained simultaneously even by X-ray diffraction, using the nonlinear least squares method. On the other hand, in the conventional stress analysis technique that has been widely used, methods different from nonlinear least squares are employed to avoid large errors attributed to the error contained in  $d_0$ , as mentioned below.

The reason why large errors are contained in the results calculated by Eq. (1) using the value  $d_{0(k)}$  that contains errors is that the strains containing an error, (expressed by  $\varepsilon_{\varphi\psi(k)} = \varepsilon_{\varphi\psi} + \Delta_{\varepsilon(k)}$ ) are used in the left-hand side of Eq. (1). To avoid this,  $\Delta_{\varepsilon(k)}$  should also be added to the right-hand side of Eq. (1) as a variable term. This workaround is explicitly carried out by the 2D method<sup>(2)</sup>. In this method, a variable term, which represents the error contained in strains attributed to the errors of  $d_0$ , is called a ‘‘pseudohydrostatic stress’’ and is treated as a component of stresses. In contrast, there are also several methods that implicitly use this type of error term, such as the  $\sin^2\psi$  method, which is widely used for the evaluation of biaxial stress state. If a stress state is assumed to be a biaxial state and a measurement is performed at  $\varphi=0$ , Eq. (1) becomes

$$\varepsilon_{\varphi\psi} = \frac{1}{2} S_2 \sigma_{11} \sin^2 \psi + S_1 (\sigma_{11} + \sigma_{22}) \quad (14)$$

On the other hand,  $\varepsilon_{\varphi\psi}$  is expressed by the following equation using a diffraction angle  $2\theta_{\varphi\psi}$  with a d-value  $d_{\varphi\psi}$  and the diffraction angle in the strain-free condition  $2\theta_0$ :

$$\varepsilon_{\varphi\psi} = \frac{d_{\varphi\psi} - d_0}{d_0} \cong -\frac{2\theta_{\varphi\psi} - 2\theta_0}{2 \tan \theta_0} \quad (15)$$

According to Eq. (14) and (15), the diffraction angle  $2\theta_{\varphi\psi}$  in the  $\varphi$  and  $\psi$  directions is defined by

$$2\theta_{\varphi\psi} \cong -S_2 \tan \theta_0 \sigma_{11} \sin^2 \psi - 2S_1 \tan \theta_0 (\sigma_{11} + \sigma_{22}) \quad (16)$$

In stress calculations using the  $\sin^2\psi$  method,  $\sigma_{11}$  is calculated from only the slope of a straight line that approximates a plot of  $2\theta_{\varphi\psi}$  versus  $\sin^2\psi$ ; therefore,  $2\theta_0$  including errors has no influence on the slope of the approximation line since the second and later terms on the right-hand side of Eq. (16) are combined as an independent variable. This operation has an equivalent effect of adding the error term of strains in the equation. This technique allows the  $\sin^2\psi$  method to avoid large errors attributed to the errors of  $d_0$ ; however, the calculation with the slope requires  $\tan \theta_0$ , which eventually causes errors.

### 3. Direct Refinement Solution (DRS) method

#### 3.1. The purpose for developing the DRS method

The DRS (Direct Refinement Solution) method has been developed to constantly obtain reliable results under a variety of circumstances. In order to achieve this purpose, the following requirements must be satisfied.

(a) High-precision stress analysis is possible even when

an exact value of  $d_0$  is unknown

Although conventional stress analysis techniques can also calculate stress values, avoiding large errors attributed to the errors of  $d_0$  as mentioned in the previous section, it is a first-order approximation under the assumption that the error rate  $\Delta_{\varepsilon(k)}$  of  $d_0$  is sufficiently small. Then, the errors may not be negligible depending on the given value of  $d_0$ .

(b) The optimal value of  $d_0$  can be obtained

It is important for researchers to obtain the actual value of  $d_0$  for evaluating stress calculation results.

In order to satisfy the above requirements, the value of  $d_0$  and the components of stress tensors except  $\sigma_{33}$  are calculated by solving the nonlinear Eq. (9) derived directly from Eq. (1), which most faithfully represents the relationship between stress and strain for isotropic elastic bodies.

### 3.2. Calculation method

The nonlinear Eq. (9) can also be solved by using the typical method, Newton's method or the Gauss-Newton method. However, with these methods, initial values must be estimated for all variables, which is very complicated. Instead of that process, the DRS method employs a less-complicated but more effective calculation method in which only the value of  $d_0$  is improved. If  $d_{0(k)}$  containing an error is used in place of this  $d_0$ , and also the error term  $\Delta_{\varepsilon(k)}$  is added in the right-hand side, the equation is given by

$$d_{\varphi\psi} = d_{0(k)} \left\{ \varepsilon_{\varphi\psi} \left( \sigma_{ij(k)} \right) + \Delta_{\varepsilon(k)} + 1 \right\} \quad (17)$$

where, the value of  $d_{0(k)}$  is a constant. Then, the value  $d_{0(k+1)}$  improved from  $d_{0(k)}$  can be calculated using the  $\Delta_{\varepsilon(k)}$  obtained by Eq. (17) as below.

$$d_{0(k+1)} = d_{0(k)} \left( 1 + \Delta_{\varepsilon(k)} \right) = d_0 \left( 1 + \Delta_{\varepsilon(k)} + \Delta_{\varepsilon(k)} + \Delta_{\varepsilon(k)} \Delta_{\varepsilon(k)} \right) \quad (18)$$

From Eq. (18), the error rate  $\Delta_{\varepsilon(k+1)}$  of  $d_{0(k+1)}$  is provided by

$$\Delta_{\varepsilon(k+1)} = \Delta_{\varepsilon(k)} + \Delta_{\varepsilon(k)} + \Delta_{\varepsilon(k)} \Delta_{\varepsilon(k)} \quad (19)$$

where  $\Delta_{\varepsilon(k)} \cong -\Delta_{\varepsilon(k)}$ ,  $|\Delta_{\varepsilon(k)}| < 1$ , and thus  $|\Delta_{\varepsilon(k+1)}| < |\Delta_{\varepsilon(k)}|$ . In other words,  $\Delta_{\varepsilon(k)}$  will converge to zero after  $d_{0(k)}$  is gradually improved by repeating the operation with Eq. (18) and, thereby, the stress value can be obtained using the optimal value of  $d_0$  and this operation. Such repetitive calculations converge rapidly. For example, if one of  $d_{\varphi\psi}$  obtained by a measurement is given as an initial value of  $d_{0(k)}$ ,  $\Delta_{\varepsilon(k)}$  will converge promptly after repeating the calculation a few times. It becomes possible to analyze all stress states, including triaxial stress states, without obtaining information on  $d_0$  beforehand.

In the actual calculation, Eq. (1), which represents the relationship between stress and strain,  $\varepsilon_{\varphi\psi}$ , can be changed as follows:

First, define  $\xi_{11}, \xi_{22}$  as

$$\begin{aligned} \xi_{11} &= \sigma_{11} - \sigma_{33} \\ \xi_{22} &= \sigma_{22} - \sigma_{11} \end{aligned} \quad (20)$$

Assign these values to Eq. (1) as below

$$\begin{aligned} \varepsilon_{\varphi\psi} &= \frac{1}{2} S_2 \left\{ \left( \xi_{11} + \sigma_{12} \sin 2\varphi + \xi_{22} \sin^2 \varphi \right) \sin^2 \psi \right. \\ &\quad \left. + \left( \sigma_{13} \cos \varphi + \sigma_{23} \sin \varphi \right) \sin 2\psi + \sigma_{33} \right\} \\ &\quad + S_1 \left( 2\xi_{11} + \xi_{22} + 3\sigma_{33} \right) \end{aligned} \quad (21)$$

Then, apply this to Eq. (17)

$$\begin{aligned} d_{\varphi\psi} &= d_{0(k)} \left[ \frac{1}{2} S_2 \left\{ \left( \xi_{11(k)} + \sigma_{12(k)} \sin 2\varphi + \xi_{22(k)} \sin^2 \varphi \right) \sin^2 \psi \right. \right. \\ &\quad \left. \left. + \left( \sigma_{13(k)} \cos \varphi + \sigma_{23(k)} \sin \varphi \right) \sin 2\psi + \sigma_{33} \right\} \right. \\ &\quad \left. + S_1 \left( 2\xi_{11(k)} + \xi_{22(k)} + 3\sigma_{33} \right) + \Delta_{\varepsilon(k)} + 1 \right] \end{aligned} \quad (22)$$

Since both  $\sigma_{33}$  and  $\Delta_{\varepsilon(k)}$  are invariable with respect to  $\varphi, \psi$  in this equation, it cannot be solved using these two values as variables. As previously mentioned, if  $\sigma_{33}$  can be regarded as zero or a small constant in the stress states where X-ray diffraction can observe, Eq. (22) will be solved by assuming a linear equation using  $\Delta_{\varepsilon(k)}$  as a variable, then repeatedly calculating the value  $d_{0(k+1)}$  improved from  $d_{0(k)}$  using the obtained  $\Delta_{\varepsilon(k)}$ .

The advantage of this form is to fix only a few variables, which enables the calculations of different stress states as follows:

(a) Triaxial stress state ( $\sigma_{33}$  is zero or a small constant)

All of  $\xi_{11}, \xi_{22}, \sigma_{23}, \sigma_{13}, \sigma_{12}, \Delta_{\varepsilon(k)}$  are variables.

(b) Biaxial stress state

$\xi_{11}, \xi_{22}, \sigma_{12}, \Delta_{\varepsilon(k)}$  are variables when  $\sigma_{23} = \sigma_{13} = 0$ .

(c) Equi-biaxial stress state

$\xi_{11}, \Delta_{\varepsilon(k)}$  are variables when  $\sigma_{23} = \sigma_{13} = \xi_{22} = \sigma_{12} = 0$ .

### 3.3. When $\sigma_{33}$ cannot be regarded as zero or a small constant

When the stress tensors  $\sigma_{23}, \sigma_{13}$  are large,  $\sigma_{33}$  is also considered to be a large value that is not negligible due to the stress curve in the depth direction. In such cases, if there are any other means to estimate  $d_0$ , all components of the stress tensor can be determined by repeating the calculation with the DRS method to continuously change the value of  $\sigma_{33}$  until  $d_0$  is coincident with the value estimated by other means. In other words, in the case where  $\sigma_{23}, \sigma_{13}$  are large and  $\sigma_{33}$  is also a large value that is not negligible, it is possible to analyze the triaxial stress state that contains  $\sigma_{33}$  with the DRS method, using the value of  $d_0$  estimated by other means.

### 3.4. Application of DRS method to single exposure technique

As mentioned above, since the DRS method is a technique to calculate stresses from  $d_{\varphi\psi}$ , it is applicable to not only X-ray diffraction patterns obtained by goniometers but also from two-dimensional X-ray diffraction images. In this section, a processing for applying the DRS method to the single-exposure technique is described.

In the single-exposure technique, X-ray diffraction

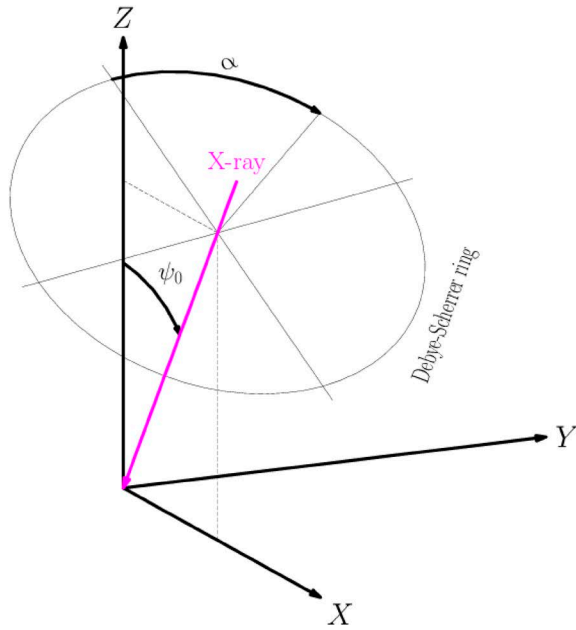


Fig. 3. Single exposure.

images are obtained using the X-rays incident at the  $\psi_0$  angle with respect to the Z axis and a two-dimensional detector located at the orthogonal position as shown in Fig. 3. At this moment, the scattering vector  $\vec{S}$  at  $\alpha$  which is the angle around Debye-Scherrer rings, is represented by the following:

$$\begin{aligned} \vec{S} &= \begin{pmatrix} S_x \\ S_y \\ S_z \end{pmatrix} \\ &= \begin{pmatrix} \cos\theta & 0 & \sin\theta \\ 0 & 1 & 0 \\ -\sin\theta & 0 & \cos\theta \end{pmatrix} \cdot \begin{pmatrix} \cos\alpha & \sin\alpha & 0 \\ -\sin\alpha & \cos\alpha & 0 \\ 0 & 0 & 1 \end{pmatrix} \\ &\quad \cdot \begin{pmatrix} \cos\psi_0 & 0 & \sin\psi_0 \\ 0 & 1 & 0 \\ -\sin\psi_0 & 0 & \cos\psi_0 \end{pmatrix} \cdot \begin{pmatrix} -1 \\ 0 \\ 0 \end{pmatrix} \\ &= \begin{pmatrix} \sin\psi_0 \sin\theta - \cos\psi_0 \cos\alpha \cos\theta \\ \sin\alpha \cos\theta \\ \cos\psi_0 \sin\theta + \sin\psi_0 \cos\alpha \cos\theta \end{pmatrix} \end{aligned} \quad (23)$$

whereas

$$S_y = \sin\varphi \sin\psi \quad (24)$$

$$S_z = \cos\psi \quad (25)$$

Based on the above, the relationship between  $\psi_0$ ,  $\alpha$ ,  $\theta$  and  $\varphi$ ,  $\psi$  is established by

$$\cos\psi = +\cos\psi_0 \sin\theta + \sin\psi_0 \cos\alpha \cos\theta \quad (26)$$

$$\sin\varphi \sin\psi = \sin\alpha \cos\theta \quad (27)$$

Using the above Eq. (26) and (27),  $\varphi$ ,  $\psi$  are calculated from  $\alpha$ ,  $\theta$  and  $\psi_0$  that were obtained by two-dimensional

diffraction images. Applying such value  $d_{\varphi\psi}$  obtained in the above manner to the DRS method, X-ray stress analyses with the high-precision single-exposure technique is realized.

In principle, the DRS method is able to analyze the triaxial stress state from a two-dimensional X-ray diffraction image; however, in reality, it has difficulty in obtaining stable analysis results because the information required for the analysis is insufficient within the range of  $\varphi$  of the scattering vectors obtained from only a single Debye-Scherrer ring due to disturbances such as electric noise from the detector. Therefore, to evaluate triaxial stress states, it is necessary to use more than one two-dimensional X-ray diffraction image obtained by rotating the sample on a stage equipped with a  $\varphi$  axis.

### 3.5. Verification of calculation accuracy by simulations

This section explains an example of how an original stress and  $d_0$  can be reproduced by processing peak lists calculated from appropriately given stress tensors with the DRS method.

The peak list in Table 1 was calculated using Eq. (1) at  $\varphi=0^\circ, 45^\circ, 90^\circ, 180^\circ, 225^\circ, 270^\circ$ , with the following given values of the stress tensor, the X-ray wavelength  $\lambda$ , the d-value in a strain-free condition  $d_0$ , and the X-ray elastic constant  $E, \nu$ .

$$\sigma_{11} = -300, \sigma_{22} = -350, \sigma_{33} = 0, \sigma_{23} = 45, \sigma_{13} = 30, \sigma_{12} = 80 \\ \lambda = 2.291045, d_0 = 1.1701213, E = 223300, \nu = 0.276$$

Table 1 shows the calculated  $2\theta$  values to seven decimal places. This indicates that the accuracy of the calculation is determined not by the algorithm of the DRS method but by the accuracy of the given data. In the calculation, a value “1.1709818242698” that was calculated from a diffraction angle appropriately selected from Table 1 was used as  $d_0$ . The values of the X-ray wavelength  $\lambda$  and the X-ray elastic constant  $E, \nu$  were used “as is” from those used in creating Table 1. The value of  $\sigma_{33}$  was given as zero. Table 2 shows the calculation results, which indicate that both the stress tensors and  $d_0$  are almost completely reproduced.

Table 3 is provided to show that a reasonable calculation result can be obtained even from a lower-precision peak list. In Table 3,  $\varphi=0^\circ, 120^\circ, 240^\circ$  is given, and the  $2\theta$  values are rounded off to three decimal places. The values of  $d_0$ , X-ray wavelength  $\lambda$ , and X-ray elastic constant  $E, \nu$  are the same as those used in calculating the peak list in Table 1.

Table 4 shows the calculation result based on the lower-precision peak list. This result indicates that a high-speed, high-precision triaxial stress analysis system is realized by applying the DRS method to three X-ray diffraction images obtained by the combination of an X-ray diffractometer employing the single-exposure technique and a sample stage containing a  $\varphi$  axis.

Table 5 is a peak list created for comparison with the  $\sin^2\psi$  method. In the calculation of the  $2\theta$  values in Table 5,  $\sigma_{23}=0, \sigma_{13}=0$  are assumed. The values of  $d_0$ ,

**Table 1.** A high-precision peak list.

$\varphi$	$\psi$	$2\theta$
0	18.435	156.0613150
0	26.565	156.1355133
0	33.211	156.2177464
0	39.232	156.3052731
0	45.000	156.3971837
45	18.435	156.0017640
45	26.565	156.0445720
45	33.211	156.1011497
45	39.232	156.1666285
45	45.000	156.2393970
90	18.435	156.0489725
90	26.565	156.1293205
90	33.211	156.2216393
90	39.232	156.3218292
90	45.000	156.4285424
180	18.435	156.1727072
180	26.565	156.2846595
180	33.211	156.3893382
180	39.232	156.4894950
180	45.000	156.5860113
225	18.435	156.1985302
225	26.565	156.3078250
225	33.211	156.4037840
225	39.232	156.4912802
225	45.000	156.5718969
270	18.435	156.2161777
270	26.565	156.3533554
270	33.211	156.4795762
270	39.232	156.5989546
270	45.000	156.7128076

**Table 2.** Calculation result based on the high-precision peak list.

$d_0$	1.1701213
$\sigma_{11}$	-299.999999999722
$\sigma_{22}$	-349.999999998969
$\sigma_{23}$	45.0000000001673
$\sigma_{13}$	29.9999999998479
$\sigma_{12}$	80.0000000020899

**Table 3.** A low-precision peak list.

$\varphi$	$\psi$	$2\theta$
0	18.435	156.061
0	26.565	156.136
0	33.211	156.218
0	39.232	156.305
0	45.000	156.397
120	18.435	156.105
120	26.565	156.217
120	33.211	156.335
120	39.232	156.458
120	45.000	156.584
240	18.435	156.207
240	26.565	156.325
240	33.211	156.428
240	39.232	156.523
240	45.000	156.612

**Table 4.** Calculation result based on the low-precision peak list.

$d_0$	1.170121198130883
$\sigma_{11}$	-299.6485468580708
$\sigma_{22}$	-350.6557612434673
$\sigma_{23}$	44.87920358674058
$\sigma_{13}$	29.81933804971606
$\sigma_{12}$	79.76226621926422

**Table 5.** A peak list for the comparison with  $\sin^2\psi$  method.

$\varphi$	$\psi$	$2\theta$
0	18.435	156.117
0	26.565	156.210
0	33.211	156.303
0	39.232	156.397
0	45.000	156.491
45	18.435	156.100
45	26.565	156.176
45	33.211	156.252
45	39.232	156.328
45	45.000	156.405
90	18.435	156.132
90	26.565	156.241
90	33.211	156.350
90	39.232	156.460
90	45.000	156.570

X-ray wavelength  $\lambda$ , and X-ray elastic constant  $E$ ,  $\nu$  are the same as those used in calculating the other peak lists. When “ $\varphi=0^\circ$ ” in Table 5 is processed with the  $\sin^2\psi$  method, the following result is obtained:

$$\sigma_{11} = -299.5082427806274$$

In the same manner, when “ $\varphi=90^\circ$ ” in Table 5 is processed with the  $\sin^2\psi$  method, this result is obtained:

$$\sigma_{22} = -350.1883127312955$$

$\tan\theta_0$  in these calculations was calculated from the  $d_0$  used in creating the peak list of Table 5.

On the other hand, with the DRS method,  $d_0=1.1709818242698$  is given in the same manner as the calculations of the other peak lists, and it results in

$$\sigma_{11} = -299.7712327491961, \sigma_{22} = -349.8650616413991, \\ \sigma_{12} = 79.88424711469493, d_0 = 1.170121794656159$$

These results show that the DRS method is able to obtain calculation results equivalent to those obtained by the  $\sin^2\psi$  method.

#### 4. Verification of measurement results compared with the conventional $\sin^2\psi$ method

In order to verify compatibility with the  $\sin^2\psi$  method, we compared the measurement results of

**Table 6.** Comparison with the measurement results using the  $\sin^2\psi$  method.

Sample	$\sin^2\psi$ method	DRS method
Steel powder	1.4 MPa	0.5 MPa
SK85 (JIS) Heat treatment material	-115.6 MPa	-116.6 MPa
SUS420J2 (JIS) Blast treatment material	-483.0 MPa	-494.7 MPa
Coil spring	-689.3 MPa	-687.1 MPa
Gear tooth face SP treatment material	-1379.0 MPa	-1380.5 MPa

the DRS method and the  $\sin^2\psi$  method for several prepared samples. Both measurements were conducted under the same measurement conditions with typical

steel samples. For the measurements using the  $\sin^2\psi$  method, the AutoMATE II micro-area X-ray stress analyzer was used, while those for the DRS method used the SmartSite RS portable X-ray stress analyzer. Table 6 shows the measurement results. For all prepared samples, the DRS method obtained measurement results equivalent to those of the conventional method, which indicates that the DRS method is compatible with the conventional method.

#### 5. Conclusion

The DRS method assumes states similar to stress states on an actual material surface, and obtains optimal solutions by improving a given  $d$ -value in the strain-free condition  $d_0$ . This allows the elimination of errors attributed to errors of  $d_0$  from stress calculation values as much as possible. In other words, the DRS method is a stress analysis method that improves the accuracy in stress calculations without requiring exact values of  $d_0$ . Moreover, when the single-exposure technique is applied to the DRS method with no goniometer, stresses can be analyzed from only one two-dimensional diffraction image, which leads to a reduction in the measurement time. Furthermore, triaxial stress analysis applying the single-exposure technique is also feasible if sufficient information required for evaluating triaxial stress states can be obtained by using a stage equipped with the  $\varphi$  axis, etc.

In the case of the biaxial or equi-biaxial states, analyses can be realized by fixing several stress tensors if required.

Therefore, the DRS method is a versatile stress analysis method that can conduct stress analyses, assuming the most suitable stress state for the measurement sample.

After comparing the results with the conventional  $\sin^2\psi$  method, we found that this method is compatible with it, which leads to the conclusion that stress analyses with the DRS method are as reliable as those of the conventional method.

#### References

- (1) The Society of Materials Science, Japan: *Standard Method for X-ray Stress Measurement*, (2002), JSMS-SD-5-02.
- (2) B. B. He: *Two-Dimensional X-Ray Diffraction*, John Wiley & Sons, Inc., (2009), 249–328.
- (3) U. Welzel, J. Ligot, P. Lamparter, A. C. Vermeulen and E. J. Mittemeijer: *Journal of Applied Crystallography*, **38** (2005), 1–29.